Rapid Communications

Four-dimensional semimetals with tensor monopoles: From surface states to topological responses

Yan-Qing Zhu [1,2], Nathan Goldman,[2] and Giandomenico Palumbo[2,*]

[1]*National Laboratory of Solid State Microstructures and School of Physics, Nanjing University, Nanjing 210093, China*

[2]*Center for Nonlinear Phenomena and Complex Systems, Université Libre de Bruxelles, Code Postal 231, Campus Plaine, B-1050 Brussels, Belgium*

(Received 9 June 2020; revised 31 July 2020; accepted 3 August 2020; published 13 August 2020)

Quantum anomalies offer a useful guide for the exploration of transport phenomena in topological semimetals. In this work, we introduce a model describing a semimetal in four spatial dimensions, whose nodal points act like tensor monopoles in momentum space. This system is shown to exhibit monopole-to-monopole phase transitions, as signaled by a change in the value of the topological Dixmier-Douady invariant as well as by the associated surface states on its boundary. We use this model to reveal an intriguing "4D parity magnetic effect," which stems from a parity-type anomaly. In this effect, topological currents are induced upon time modulating the separation between the fictitious monopoles in the presence of a magnetic perturbation. Besides its theoretical implications in both condensed matter and quantum field theory, the peculiar four-dimensional (4D) magnetic effect revealed by our model could be measured by simulating higher-dimensional semimetals in synthetic matter.

DOI: 10.1103/PhysRevB.102.081109

Introduction. Quantum anomalies play a central role in our understanding and applications of quantum field theories [1,2]. Given a classical action, a local symmetry is "anomalous" if it represents an obstruction to quantize the classical field theory (i.e., the corresponding path integral cannot be made invariant with respect to both gauge symmetry and the anomalous symmetry). In high-energy physics, this obstruction prevents the existence of quantum field theories with certain symmetries, which can be cured by introducing anomaly-cancellation effects into the description [3]. Such anomalous situations can, however, give rise to observable phenomena, such as the chiral magnetic effect related to the so-called chiral anomaly, as originally shown in Ref. [4] in the context of the quark-gluon plasma.

Quantum anomalies are not restricted to Lorentz-invariant systems. In particular, they also give rise to novel quantum effects in condensed matter physics [5–11]. For instance, it was shown that the chiral anomaly emerges in Weyl semimetals set out of equilibrium [12–17]. In this context, the corresponding chiral magnetic effect gives rise to quantized electric currents upon applying an external magnetic field. Another well studied anomaly is the parity anomaly [18–25], which gives rise to topological effects in two-dimensional gapless (Dirac) phases [26,27] related to the emergence of Chern-Simons theories.

Recently, parity and chiral anomalies have been explored in multiband models, in two and three dimensions, respectively [28–30]. These systems support higher-spin quasiparticles, where the Weyl-like cones become multifold degenerate [31–40]. Interestingly, the parity anomaly can also exist in four and six dimensions [41,42], which suggests relevant implications in the context of higher-dimensional synthetic topological matter [43–45]. In addition, it has been shown that a three-band model in four dimensions can give rise to a gapless topological phase characterized by a tensor monopole [46,47], whose topological nature is established by the Dixmier-Douady ($\mathcal{DD}$) invariant [48,49]. Their topological response in the presence of an electromagnetic field has remained unexplored.

The goal of this work is twofold. First, we introduce a four-dimensional lattice model that supports both gapless spin-1/2 and spin-3/2 birefringent fermions, depending on symmetries. When both CP (combined charge conjugation C and inversion P symmetries) and chiral symmetries are preserved, the Dirac cones are associated with $\mathbb{Z}_2$ monopoles in momentum space [50,51]. By breaking CP while preserving sublattice (chiral) symmetry, the topological semimetal phase is instead characterized by the $\mathcal{DD}$ invariant in the bulk, which one can associate to fictitious tensor monopoles [46,47]. This represents a monopole-to-monopole topological phase transition. We show the presence of topologically protected Fermi arcs on the three-dimensional boundary, and describe their modification across the transition. Secondly, we identify a novel quantum effect, coined "parity magnetic effect," which arises in the presence of a magnetic field and can be attributed to a parity anomaly. This is a peculiar topological effect associated to the existence of quantized topological currents in four-dimensional (4D) semimetals. This effect could be measured in quantum-engineered settings using a synthetic dimension [52–54].

4D topological semimetals. We start by considering a four-band Hamiltonian for spinless fermions on a four-dimensional lattice. The corresponding momentum-space Hamiltonian is given by

$$H(\boldsymbol{k}) = d_x\tilde{\Gamma}_x + d_y\tilde{\Gamma}_y + d_z\tilde{\Gamma}_z + d_w\tilde{\Gamma}_w, \tag{1}$$

*giandomenico.palumbo@gmail.com

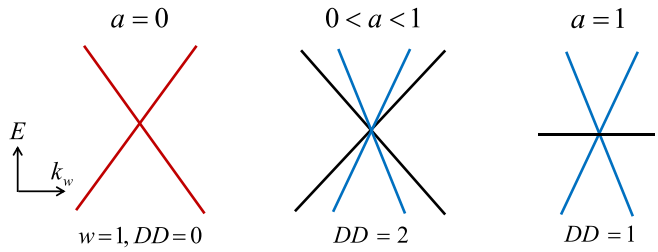

FIG. 1. Monopole-to-monopole transition: Schematic spectra $E(k_w)$ of H_+ at $k_{x,y,z}=0$. When $a=0$, the twofold degenerate spectrum (red) hosts a $\mathbb{Z}_2$ monopole with winding number $w=1$. For $a\neq 0,\pm 1$, the degeneracy is lifted and the nodal point hosts a tensor monopole captured by a nonzero $\mathcal{DD}$ invariant: $\mathcal{DD}=2$. When $a=\pm 1$, the two middle bands become perfectly flat (black) and the low-energy band (blue) contributes to $\mathcal{DD}=1$.

with the four-component Bloch vector defined as

$$d_x = 2J\sin k_x,\ d_y = 2J\sin k_y,\ d_z = 2J\sin k_z,$$
$$d_w = 2J(M-\cos k_x-\cos k_y-\cos k_z-\cos k_w). \quad (2)$$

Here J is the hopping amplitude on the 4D lattice, M is a tunable parameter, and the 4×4 matrices $\tilde{\Gamma}_i$ read

$$\tilde{\Gamma}_x=\sigma_0\otimes\sigma_1+a\sigma_1\otimes\sigma_0,\quad \tilde{\Gamma}_y=\sigma_2\otimes\sigma_3+a\sigma_3\otimes\sigma_2,$$
$$\tilde{\Gamma}_z=\sigma_0\otimes\sigma_2+a\sigma_2\otimes\sigma_0,\quad \tilde{\Gamma}_w=\sigma_1\otimes\sigma_3+a\sigma_3\otimes\sigma_1,$$

where σ_i are Pauli matrices and a is a constant parameter. These matrices only satisfy the Clifford algebra for $a=0$ ("Dirac regime"). When $a\neq 0$, the Hamiltonian (1) supports spin-3/2 birefringent quasiparticles similarly to previous models in lower dimensions [32,33,35,36,39]. In addition, this Hamiltonian preserves a chiral (sublattice) symmetry, $\{S,H\}=0$ with $S=\sigma_3\otimes\sigma_3$. Its spectrum reads

$$E(\boldsymbol{k})=\pm(1\pm a)\sqrt{d_x^2+d_y^2+d_z^2+d_w^2}. \quad (3)$$

Notice that the two middle bands become perfectly flat when $a=\pm 1$ (Fig. 1). For $2<M<4$ and $a\neq 0$, there exists a single pair of Dirac-like cones in the first Brillouin zone (BZ) separated along the k_w axis and located at $\boldsymbol{K}_\pm=(0,0,0,\pm\arccos k_m)$ with $k_m=M-3$. For convenience and without loss of generality, we focus on the low-energy effective Hamiltonians near the nodal points $\boldsymbol{K}_\pm=(0,0,0,\pm\pi/2)$ for $M=3$,

$$H_\pm(\boldsymbol{q})=vq_{\pm,x}\tilde{\Gamma}_x+vq_{\pm,y}\tilde{\Gamma}_y+vq_{\pm,z}\tilde{\Gamma}_z\pm vq_{\pm,w}\tilde{\Gamma}_w, \quad (4)$$

where $v=2J$ with $J>0$ and the effective momenta $\boldsymbol{q}_\pm=\boldsymbol{k}-\boldsymbol{K}_\pm$. When $a=0$, the Dirac cones are protected by combined CP symmetry, $\{CP,H\}=0$, where $CP=\sigma_1\otimes\sigma_2\hat{K}$, $\hat{K}$ is the complex conjugate, and $(CP)^2=-1$. Thus, they behave like monopoles carrying a $\mathbb{Z}_2$ charge, as studied in Ref. [50]. For $a\neq 0$, the combined CP symmetry is broken and the Hamiltonian (1) only preserves chiral symmetry. In this regime, the system belongs to class AIII and the nodal points behave like tensor monopoles, which are characterized by a $\mathbb{Z}$ invariant [46,47]. Our model thus exhibits a monopole-to-monopole phase transition upon tuning a (see Fig. 1). In our 4×4 representation, there only exists a single mass term (proportional to $\sigma_3\otimes\sigma_3$) that breaks CP and opens a bulk gap; however, this term simultaneously breaks the chiral symmetry S; hence, this perturbation would open a gap for both the $\mathbb{Z}_2$ and the $\mathbb{Z}$ cases. The situation would be different in an 8×8 representation, where there exists a mass term that breaks S without breaking CP [55].

We now further characterize these two types of monopoles, by focusing on H_+ in Eq. (4). Since the Hamiltonian preserves chiral (sublattice) symmetry in both regimes, one can calculate the winding number associated with the mapping $\boldsymbol{q}\backslash\{0\}\in\mathbb{S}^3\to\mathbf{d}/|\mathbf{d}|\in\mathbb{S}^3$, where the three-dimensional unit sphere $\mathbb{S}^3$ encloses the monopole in q space. The corresponding winding number is given by [56–58]

$$w=\frac{1}{12\pi^2}\int_{\mathbb{S}^3}dq^\mu\wedge dq^\nu\wedge dq^\rho\epsilon^{ijkl}\frac{1}{|d|^4}d_i\partial_\mu d_j\partial_\nu d_k\partial_\rho d_l, \quad (5)$$

with $d_i=vq_i$. Importantly, we obtain $w=1$ for both types of monopoles, which indicates that this winding number is not able to distinguish between the different topological-semimetal phases of our model. In order to solve this issue, we employ the $\mathcal{DD}$ invariant, which is zero in the CP-symmetric "Dirac" regime ($a=0$), while it is nonzero in class AIII [46,47]. This invariant can be expressed as

$$\mathcal{DD}=\frac{1}{2\pi^2}\int_{\mathbb{S}^3}dq^\mu\wedge dq^\nu\wedge dq^\rho\sum_{n=1,2}\mathcal{H}^n_{\mu\nu\rho}, \quad (6)$$

where

$$\mathcal{H}^n_{\mu\nu\rho}=\partial_\mu B^n_{\nu\rho}+\partial_\nu B^n_{\rho\mu}+\partial_\rho B^n_{\mu\nu} \quad (7)$$

denotes the three-form Berry curvature associated with the nth eigenstate $|u_n(\boldsymbol{q})\rangle$; here, only the two lowest bands ($n=1,2$) contribute to the $\mathcal{DD}$ invariant, as required by the half-filling condition. The two-form tensor Berry connection $B^n_{\mu\nu}$ in Eq. (7) is defined as [47]

$$B^n_{\mu\nu}=\phi_n\mathcal{F}^n_{\mu\nu},\quad \phi_n=-\frac{i}{2}\log\prod_{\aleph=1}^{4}u_n^\aleph, \quad (8)$$

where $\mathcal{F}^n_{\mu\nu}=\partial_\mu\mathcal{A}^n_\nu-\partial_\nu\mathcal{A}^n_\mu$ is the Berry curvature, $\mathcal{A}^n_\mu=\langle u_n|i\partial_\mu|u_n\rangle$ is the Berry connection ($\partial_\mu\equiv\partial_{q_\mu}$), and $u_n^\aleph$ denotes the components of $|u_n\rangle$. We find $\mathcal{DD}=2$ for $a\neq 0,\pm 1$, noting that each of the two lowest bands contributes a charge $+1$. The monopole-to-monopole transition, which is signaled by a change in the value of the $\mathcal{DD}$ invariant, is illustrated in Fig. 1. In addition, for the critical flatband case ($a=\pm 1$), a single nondegenerate low-energy band contributes, thus yielding $\mathcal{DD}=1$ [46]. One also verifies that the monopoles described by H_- carry the opposite tensor charge.

Surface states. To further investigate the topological properties of the semimetal Hamiltonian (1), we now study the surface energy spectra for $M=3$, upon applying open boundary conditions along the z direction. As sketched in Fig. 2(a), the zero-energy surface states depict a degenerate Fermi arc (colored in red) connecting two monopoles of opposite charges. The origin of this Fermi arc can be understood from two perspectives, as we now explain.

A first viewpoint is obtained by fixing k_w and by studying the surface modes of the resulting three-dimensional (3D) gapped subsystem. Upon taking such a slice, the 3D

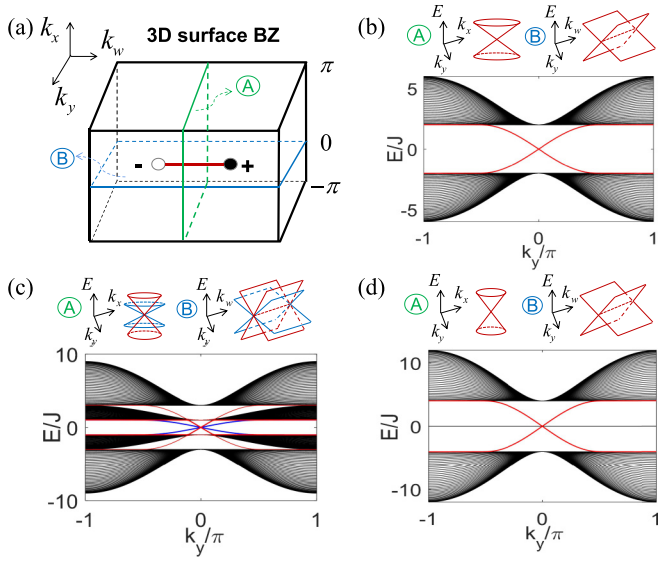

FIG. 2. Surface spectra of the model (1) upon applying open boundary conditions along z. (a) Sketch of the zero-energy Fermi arc within the 3D BZ. Numerical surface spectra at $k_x = k_w = 0$ are shown for (b) $a = 0$, (c) $a = 0.5$, and (d) $a = 1$. The diagrams labeled by A (respectively, B) depict the surface spectra of the 3D topological insulator $H|_{k_w=0}$ (respectively, the surface spectra of the 3D gapless semimetal $H|_{k_x=0}$). In (c) the red (respectively, blue) spectra correspond to the boundary at $z = 1$ (respectively, $z = L_z$). Here we set $L_z = 40$.

Hamiltonian $H|_{k_w=k_w^0}$ can either describe a $\mathbb{Z}_2$ topological insulator ($a = 0$) or a chiral topological insulator ($a \neq 0$) [56,58–61]. We find different regimes as a function of k_w^0: the 3D subsystem is nontrivial [with $\mathbb{Z}_2$ index $w = 1$ for $a = 0$, and $\mathbb{Z}$-valued $\mathcal{DD} = 2$ ($\mathcal{DD} = 1$) for $a \neq 0, \pm 1$ ($a = \pm 1$)], within the range $k_w^0 \in (-\pi/2, \pi/2)$, and trivial otherwise. Here, the topological invariants are calculated using Eq. (5) for $a = 0$ and Eq. (6) for $a \neq 0$, upon replacing $\mathbb{S}^3$ by the 3D BZ $\mathbb{T}^3$. These 3D topological insulators host 2D Dirac boundary states, whose dispersion is defined over the A plane shown in Fig. 2(a); their zero-energy nodal point forms a degenerate line along the k_w axis, i.e., a Fermi arc connecting the two monopoles.

Another viewpoint consists in taking a slice at fixed $k_x = 0$ (or $k_y = 0$). The resulting subsystem $H|_{k_x=0}$ forms a gapless metallic phase, which is similar to the (real) Dirac semimetal [51] for $a = 0$. Its dispersion, defined over the B surface in Fig. 2(a), consists of two inclined planes, whose zero-energy crossing line forms a Fermi arc connecting the two monopoles in the bulk.

We show illustrative surface spectra in Figs. 2(b) and 2(c). For $a = 0$ [Fig. 2(b)], one obtains a Dirac cone over the A plane and two inclined planes over the B plane. Note that these spectra are twofold degenerate, as they describe the surface states on both boundaries (at $z = 1$ and $z = L_z$). This degeneracy is then lifted upon increasing a, as shown in Fig. 2(c). When reaching $a = 1$ [Fig. 2(d)], the surface mode at $z = L_z$ vanishes into the zero-energy flat bulk band, while a single (nondegenerate) surface mode survives at $z = 1$. These surface spectra are well described by the boundary Hamiltonian [55]

$$H_{\pm}^{BS} = \pm(1 \pm a)(k_x\sigma_1 - k_y\sigma_2), \quad \text{for } k_w \in \left(-\frac{\pi}{2}, \frac{\pi}{2}\right), \tag{9}$$

which was derived from the bulk model $H(\boldsymbol{k})$ for $M = 3$; here $\pm$ refers to the boundaries at $z = 1$ and $z = L_z$, respectively. We note that the transformations of the boundary modes reflect the monopole-to-monopole transition in the bulk (Fig. 1).

Parity magnetic effect and topological currents. We now show how to derive a universal magnetic effect for our model, by calculating quantum anomalies through quantum-field-theoretical methods. In this framework, we consider the continuum limit of our 4D topological semimetal, taking into account the single pair of monopoles at $\boldsymbol{K}_{\pm}$. The resulting 8×8 effective Hamiltonian, defined in 4D momentum space, reads

$$H_{\text{eff}} = k_i\tilde{G}^i - b_\mu\tilde{G}_b^\mu, \tag{10}$$

where $i = x, y, z, w$ and $\mu = t, x, y, z, w$. Here, we introduced the dipolar momentum b_μ, which denotes the separation of the two monopoles in momentum space, with vector $\boldsymbol{b} = (\boldsymbol{K}_+ - \boldsymbol{K}_-)/2$, and in energy with offset $2b_t$; the 8×8 matrices $\tilde{G}^i$ and $\tilde{G}_b^\mu$ are defined as

$$\begin{aligned} &\tilde{G}^j = \sigma_0 \otimes \tilde{\Gamma}_j, \quad \tilde{G}^w = \sigma_3 \otimes \tilde{\Gamma}_w, \quad \tilde{G}_b^t = \sigma_3 \otimes I_4, \\ &\tilde{G}_b^j = \sigma_3 \otimes \tilde{\Gamma}_j, \quad \tilde{G}_b^w = \sigma_0 \otimes \tilde{\Gamma}_w, \end{aligned} \tag{11}$$

where $j = x, y, z$, and I_4 is the 4×4 identity matrix. By implementing a Legendre transformation on Eq. (10), the action can be written in terms of a first-order Lagrangian,

$$S[\bar{\psi}, \psi, b] = \int d^5x\, \bar{\psi}\left(i\tilde{\gamma}^\mu\partial_\mu - \tilde{\gamma}_b^\mu b_\mu\right)\psi, \tag{12}$$

where $\bar{\psi} = \psi^\dagger\tilde{\gamma}^t$, $\tilde{\gamma}^i = \tilde{\gamma}^t\tilde{G}^i$, $\tilde{\gamma}_b^\mu = \tilde{\gamma}^t\tilde{G}_b^\mu$, with $\tilde{\gamma}^t = \sigma^0 \otimes S$. In order to show the topological response of the 4D semimetal to an external electromagnetic field A_μ, we integrate out the fermion field and obtain the following effective action:

$$S_{\text{eff}} = -i \log\det\left(i\tilde{\gamma}^\mu D_\mu - \tilde{\gamma}_b^\mu b_\mu\right), \tag{13}$$

where $D_\mu = \partial_\mu - iA_\mu$ is the gauge covariant derivative. This effective action S_{eff} with zero mass needs to be regularized due to ultraviolet divergences [18]. However, the regularization explicitly breaks certain symmetries of the original action, hence giving rise to anomalies as we now show.

We use the standard Pauli-Villars method [24] to obtain the topological action in the low-energy regime, which consists in introducing a mass term $\tilde{m}\bar{\psi}\psi$ with $\tilde{m} = m - \alpha k^2$. To reveal the "parity" anomaly [62], we first consider the Dirac case ($a = 0$); we determine the effective Chern-Simons action, by calculating a one-loop triangle diagram [55,63], and we obtain

$$S_{\text{top}} = \frac{C_2}{4\pi^2}\int d^5x\, \epsilon^{\mu\nu\lambda\rho\sigma} b_\mu\partial_\nu A_\lambda\partial_\rho A_\sigma, \tag{14}$$

where $C_2 = -[\text{sgn}(m) + \text{sgn}(\alpha)]/2$ is nothing but the second Chern number of the gapped system described by H_+ with the regularized mass $\tilde{m}$ [27,64,65]. The presence of a second Chern number in the description of a 4D semimetal is analog to the appearance of the first Chern number in 2D topological semimetals [26,27].

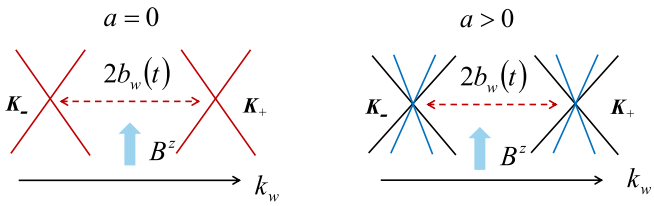

FIG. 3. The parity magnetic effect: A topological current J^z can be induced by a pair of 4D monopoles upon modulating the monopole separation $b_w(t)$ in the presence of a weak magnetic field B^z [see Eq. (16)].

We find that a similar calculation [55] can be performed for the spin-3/2 case ($a \neq 0, \pm 1$), yielding the same topological action in Eq. (14). In that case, the anomaly takes the form of a "4D sublattice anomaly," which shares features of the 4D parity anomaly [66]. In the flatband limit ($a = \pm 1$), the system remains gapless in the presence of the mass $\tilde{m}$; in this case, C_2 diverges, and the topological action is ill-defined.

Based on these results, we find that the topological response current is universal for both spin-1/2 and spin-3/2 birefringent quasiparticles, and it is given by

$$J^\mu = \frac{\delta S_{\text{top}}}{\delta A_\mu} = \frac{C_2}{2\pi^2}\epsilon^{\mu\nu\lambda\rho\sigma}\partial_\nu b_\lambda \partial_\rho A_\sigma . \tag{15}$$

This result describes the "parity magnetic effect" exhibited by our 4D-semimetal model, as we now further illustrate. For concreteness, let us consider the response of our system to a static and uniform magnetic field (i.e., $A_y = xB^z$ and $A_{x,z,w,t} = 0$), and to a simultaneous time-dependent modulation of the cones separation, $b_w = \arccos[M(t) - 3]$ (see Fig. 3). In this case, a single component of the Faraday tensor ($F_{xy} = B^z$) contributes to Eq. (15), which yields the topological response

$$J^z = \frac{C_2}{2\pi^2}(\partial_t b_w)B^z. \tag{16}$$

In this effect, the separation vector b_w plays the role of an effective axial gauge field [67], whose time dependence induces an effective electric field $E_w = \partial_t b_w$. The "parity magnetic effect" in Eq. (16) constitutes a central result of this work; it represents a unique topological response of 4D gapless topological phases, in direct analogy with the chiral magnetic effect exhibited by 3D Weyl semimetals [12–17].

We note that the parity magnetic effect in Eq. (16) could be experimentally studied in 3D quantum-engineered setups extended by a synthetic dimension [53], as could be realized for cold atoms in optical lattices [68], for photons in arrays of ring resonators [54], or in electric circuits [69]. The time-varying component $b_w(t)$ could be induced through a periodic driving of an on-site coupling, as proposed in Ref. [26] for a 2D-semimetal setting.

Finally, one may wonder whether the $\mathcal{DD}$ invariant, which characterizes the topology of the nodal points, also plays a role in 4D magnetic effects. In 3D Weyl semimetals, the chiral magnetic effect was shown to be directly related to the existence of Fermi arcs [70]. Similarly, we expect the Fermi arcs analyzed in Fig. 2 to play a similar role in 4D magnetic effects. In this framework, the $\mathcal{DD}$ invariant could constitute a key element.

Conclusions. We have introduced and analyzed a 4D semimetal model, whose nodal points can be associated to tensor monopoles characterized by the $\mathcal{DD}$ invariant. The system has topological Fermi arcs on its boundary, which are protected by the sublattice (chiral) symmetry. This model reveals a novel type of topological response, the parity magnetic effect, according to which a topological current can be induced by combining a magnetic perturbation with a time modulation of the band structure. Our results expand our knowledge of quantum anomalies and their corresponding physical effects in higher-dimensional topological phases of matter, and they suggest interesting explorations in synthetic matter.

Acknowledgments. We thank Shi-Liang Zhu for helpful discussions. Work in Brussels is supported by the FRS-FNRS and the ERC through the Starting Grant project TopoCold. Y.Q.Z. also acknowledges financial support from the China Scholarship Council.

[1] R. A. Bertlmann, *Anomalies in Quantum Field Theory* (Oxford University Press, New York, 2000).
[2] K. Landsteiner, Acta Phys. Pol., B **47**, 2617 (2016).
[3] I. Garcia-Etxebarria and M. Montero, J. High Energy Phys. (2019) 3.
[4] K. Fukushima, D. E. Kharzeev, and H. J. Warringa, Phys. Rev. D **78**, 074033 (2008).
[5] D. T. Son and N. Yamamoto, Phys. Rev. Lett. **109**, 181602 (2012).
[6] M. N. Chernodub, A. Cortijo, A. G. Grushin, K. Landsteiner, and M. A. H. Vozmediano, Phys. Rev. B **89**, 081407(R) (2014).
[7] O. Parrikar, T. L. Hughes, and R. G. Leigh, Phys. Rev. D **90**, 105004 (2014).
[8] H. Sumiyoshi and S. Fujimoto, Phys. Rev. Lett. **116**, 166601 (2016).
[9] Z.-M. Huang, J. Zhou, and S.-Q. Shen, Phys. Rev. B **96**, 085201 (2017).
[10] J. Nissinen, Phys. Rev. Lett. **124**, 117002 (2020).
[11] Z.-M. Huang, B. Han, and M. Stone, Phys. Rev. B **101**, 125201 (2020).
[12] A. A. Zyuzin and A. A. Burkov, Phys. Rev. B **86**, 115133 (2012).
[13] A. G. Grushin, Phys. Rev. D **86**, 045001 (2012).
[14] M. M. Vazifeh and M. Franz, Phys. Rev. Lett. **111**, 027201 (2013).
[15] D. I. Pikulin, A. Chen, and M. Franz, Phys. Rev. X **6**, 041021 (2016).
[16] J. Behrends, S. Roy, M. H. Kolodrubetz, J. H. Bardarson, and A. G. Grushin, Phys. Rev. B **99**, 140201(R) (2019).
[17] N. P. Armitage, E. J. Mele, and A. Vishwanath, Rev. Mod. Phys. **90**, 015001 (2018).
[18] A. N. Redlich, Phys. Rev. Lett. **52**, 18 (1984).
[19] A. J. Niemi and G. W. Semenoff, Phys. Rev. Lett. **51**, 2077 (1983).

[20] F. D. M. Haldane, Phys. Rev. Lett. **61**, 2015 (1988).
[21] E. Witten, Phys. Rev. B **94**, 195150 (2016).
[22] M. F. Lapa, Phys. Rev. B **99**, 235144 (2019).
[23] J. Bottcher, C. Tutschku, L. W. Molenkamp, and E. M. Hankiewicz, Phys. Rev. Lett. **123**, 226602 (2019).
[24] C. Tutschku, J. Bottcher, R. Meyer, and E. M. Hankiewicz, Phys. Rev. Research **2**, 033193 (2020).
[25] M. Kurkov and D. Vassilevich, J. High Energy Phys. (2018) 72.
[26] Z. Lin, X.-J. Huang, D.-W. Zhang, S.-L. Zhu, and Z. D. Wang, Phys. Rev. A **99**, 043419 (2019).
[27] S. T. Ramamurthy and T. L. Hughes, Phys. Rev. B **92**, 085105 (2015).
[28] J. Zhou, X. Qi, Y. Wu, and S.-P. Kou, J. Phys.: Conden. Matter **32**, 405503 (2020).
[29] L. Lepori, M. Burrello, and E. Guadagnini, J. High Energy Phys. (2018) 110.
[30] R. M. A. Dantas, F. Pena-Benitez, B. Roy, and P. Surowka, Phys. Rev. Res. **2**, 013007 (2020).
[31] D. Bercioux, D. F. Urban, H. Grabert, and W. Hausler, Phys. Rev. A **80**, 063603 (2009).
[32] Z. Lan, N. Goldman, A. Bermudez, W. Lu, and P. Öhberg, Phys. Rev. B **84**, 165115 (2011).
[33] M. P. Kennett, N. Komeilizadeh, K. Kaveh, and P. M. Smith, Phys. Rev. A **83**, 053636 (2011).
[34] S. M. Young and B. J. Wieder, Phys. Rev. Lett. **118**, 186401 (2017).
[35] B. Roy, M. P. Kennett, K. Yang, and V. Juricic, Phys. Rev. Lett. **121**, 157602 (2018).
[36] B. Bradlyn, J. Cano, Z. Wang, M. G. Vergniory, C. Felser, R. J. Cava, and B. A. Bernevig, Science **353**, aaf5037 (2016).
[37] M. Ezawa, Phys. Rev. B **94**, 195205 (2016).
[38] I. C. Fulga, L. Fallani, and M. Burrello, Phys. Rev. B **97**, 121402(R) (2018).
[39] F. Flicker, F. de Juan, B. Bradlyn, T. Morimoto, M. G. Vergniory, and A. G. Grushin, Phys. Rev. B **98**, 155145 (2018).
[40] M.-A. Sánchez-Martínez, F. de Juan, and A. G. Grushin, Phys. Rev. B **99**, 155145 (2019).
[41] L. Alvarez-Gaume, S. Della Pietra, and G. Moore, Ann. Phys. **163**, 288 (1985).
[42] F. Bonetti, T. W. Grimm, and S. Hohenegger, J. High Energy Phys. (2013) 124.
[43] H. M. Price, O. Zilberberg, T. Ozawa, I. Carusotto, and N. Goldman, Phys. Rev. Lett. **115**, 195303 (2015).
[44] I. Petrides, H. M. Price, and O. Zilberberg, Phys. Rev. B **98**, 125431 (2018).
[45] C. H. Lee, Y. Wang, Y. Chen, and X. Zhang, Phys. Rev. B **98**, 094434 (2018).
[46] G. Palumbo and N. Goldman, Phys. Rev. Lett. **121**, 170401 (2018).
[47] G. Palumbo and N. Goldman, Phys. Rev. B **99**, 045154 (2019).
[48] V. Mathai and G. C. Thiang, Commun. Math. Phys. **355**, 561 (2017).
[49] M. K. Murray, J. Lond. Math. Soc. **54**, 403 (1996).
[50] Y. X. Zhao, A. P. Schnyder, and Z.-D. Wang, Phys. Rev. Lett. **116**, 156402 (2016).
[51] Y. X. Zhao and Y. Lu, Phys. Rev. Lett. **118**, 056401 (2017).
[52] H. M. Price, Phys. Rev. B **101**, 205141 (2020).
[53] T. Ozawa and H. M. Price, Nat. Rev. Phys. **1**, 349 (2019).
[54] T. Ozawa, H. M. Price, N. Goldman, O. Zilberberg, and I. Carusotto, Phys. Rev. A **93**, 043827 (2016).
[55] See Supplemental Material at http://link.aps.org/supplemental/10.1103/PhysRevB.102.081109 for details, which includes Refs. [71–74].
[56] A. P. Schnyder, S. Ryu, A. Furusaki, and A. W. W. Ludwig, Phys. Rev. B **78**, 195125 (2008).
[57] D.-W. Zhang, Y.-Q. Zhu, Y. X. Zhao, H. Yan, and S.-L. Zhu, Adv. Phys. **67**, 253 (2018).
[58] T. Neupert, L. Santos, S. Ryu, C. Chamon, and C. Mudry, Phys. Rev. B **86**, 035125 (2012).
[59] A. P. Schnyder, S. Ryu, A. Furusaki, and A. W. W. Ludwig, AIP Conf. Proc. **1134**, 10 (2009).
[60] P. Hosur, S. Ryu, and A. Vishwanath, Phys. Rev. B **81**, 045120 (2010).
[61] S.-T. Wang, D.-L. Deng, and L.-M. Duan, Phys. Rev. Lett. **113**, 033002 (2014).
[62] In the Dirac (spin-1/2) case, the "parity" anomaly actually involves a reflection symmetry, rather than the parity symmetry (which is never anomalous in our model); see [55].
[63] X.-L. Qi, T. L. Hughes, and S.-C. Zhang, Phys. Rev. B **78**, 195424 (2008).
[64] M. F. L. Golterman, K. Jansen, and D. B. Kaplan, Phys. Lett. B **301**, 219 (1993).
[65] H. Fukaya, T. Onogi, S. Yamaguchi, and X. Wu, Phys. Rev. D **101**, 074507 (2020).
[66] In the spin-3/2 case, reflection symmetry along the w direction is already broken in the Hamiltonian. To seek for an anomaly here, we need to introduce a mass regulator that breaks the sublattice (chiral) symmetry. Actually, the Pauli-Villars mass regulator adopted in the spin-1/2 case is the right choice because besides reflection, it breaks also the sublattice (chiral) symmetry for any value of the parameter a. For more details, see the Supplemental Material [55].
[67] S. Roy, M. Kolodrubetz, N. Goldman, and A. G. Grushin, 2D Mater. **5**, 024001 (2018).
[68] A. Celi, P. Massignan, J. Ruseckas, N. Goldman, I. B. Spielman, G. Juzeliunas, and M. Lewenstein, Phys. Rev. Lett. **112**, 043001 (2014).
[69] Y. Wang, H. M. Price, B. Zhang, and Y. D. Chong, Nat. Commun. **11**, 2356 (2020).
[70] P. Baireuther, J. A. Hutasoit, J. Tworzydlo, and C. W. J. Beenakker, New J. Phys. **18**, 045009 (2016).
[71] A. N. Redlich, Phys. Rev. D **29**, 2366 (1984).
[72] Y. X. Zhao and Z. D. Wang, Phys. Rev. B **89**, 075111 (2014).
[73] S.-Q. Shen, *Topological Insulators: Dirac Equation in Condensed Matters* (Springer-Verlag, Berlin/Heidelberg, 2012).
[74] S.-C. Zhang and J. Hu, Science **294**, 823 (2001).